

Equation of Motion for Pinned Fluxes at Volume Defects and Increases of a Diamagnetic Property by Flux Pinning in Superconductors

H. B. Lee, G. C. Kim, and Y. C. Kim*

Department of Physics, Pusan National University, Busan 46241, Korea

R. K. Ko and D. Y. Jeong

Korea Electrotechnology Research Institute, Changwon 51543, Korea

Abstract

Whereas there are two critical fields that are H_{c1} and H_{c2} in the ideal type II superconductor, there is another critical field H'_{c1} defined as the field showing the maximum diamagnetic property in the real type II superconductor. Here we present that H'_{c1} is able to be proved theoretically and experimentally. We have derived the equation based on the pinning effect of volume defects. MgB_2 bulks which were synthesized by Mg and B are similar to this model. The number of quantum fluxes pinned at a defect of radius r , a pinning penetration depth, the magnetic flux penetration method, and a magnetization at H'_{c1} in the static state are suggested through the equation of the model. It is speculated that fluxes pinned on volume defects in the superconductor have to be picked out from the defect and move an inside of the superconductor when the pick-out forces of pinned fluxes is larger than the pinning force of the defect ($F_{pickout} > F_{pinning}$) or when the distance between quantum fluxes pinned at a volume defect is the same as that of H_{c2} . In reality, $\Delta G_{dynamic}$ is involved for movement of pinned fluxes. When volume defects are small and many, the experimental results are closer to the calculated ones because of a small $\Delta G_{dynamic}$. However, when volume defects are large and a few, the experimental results are much lower than the calculated ones because of a large $\Delta G_{dynamic}$.

*Electronic address: yckim@pusan.ac.kr; Fax: +82-51-513-7664

I. INTRODUCTION

One of phenomena which have not been explained in superconductors is that diamagnetic property increases after H_{c1} . This is against the definition that superconductors decrease its diamagnetic property after H_{c1} . Although the increase of the diamagnetic property after H_{c1} is obvious in almost all of superconductors, superconductor researchers accept it implicitly because most of superconductors showed the general behavior superficially

Generally, it has been understood that there is H_{c1} and H_{c2} in the type II superconductor [1–4]. However, this definition is for the ideal type II superconductor. It is certain that there is H'_{c1} which is defined as the field showing maximum diamagnetic property in the real type II superconductor, because the pinning effects of defects exist in superconductor. Although many researchers have studied for the flux pinning effects, their results depend only on experimental techniques owing to the absence of proper theory [5–7]. The purpose of this paper is that H'_{c1} be acknowledged as an another critical field in the superconductor and detail mechanism would be shown.

In fact, it is not easy to indicate H_{c1} in field dependence of magnetization curves (M-H curves), whereas it is simple to indicate H'_{c1} in M-H curves, which is just the beginning point of the maximum magnetization. According to the definition of type II superconductor, M-H curve must be a straight line to H_{c1} and the diamagnetic property of the superconductor must decrease owing to flux penetration if the field increases over H_{c1} . However, all of real type II superconductor do not reduce their diamagnetic property in spite of passing over H_{c1} . They show much better diamagnetic property at H'_{c1} than H_{c1} .

Many researchers have stated that H_{c1} of MgB_2 is about 250 - 480 Oe [8, 9]. However, the maximum diamagnetic property appears at much higher fields. The behavior is carefully shown in other MgB_2 superconductors, melt-textured growth (MTG) specimens and single crystal superconductor (SCC), which can be called as a volume defect-dominating superconductor (VDS) [10–12]. The phenomenon appears not only in VDSs, but also in the planar defect-dominating superconductors (PDS) such as a high temperature superconductor (HTSC) which were made by solid state reaction method and thin films [13, 14].

A study for the increase of the diamagnetic property after H_{c1} is that the one of Bean-Livingston (B-L) is almost unique [15]. Most of superconducting single crystal (SSC) researchers have explained the increase of diamagnetic property after H_{c1} based on the study

[16, 17]. However, the phenomenon is not limited to SSC, but rather higher in bulks as mentioned. Although B-L condition (a clean surface) is unsatisfied in bulk one, there is an increase of diamagnetic property than that of H_{c1} . Thus, the effect of B-L and pinning phenomena are concurrently or competitively occurring in SSCs for the increase of diamagnetic property over H_{c1} because SSCs are not completely free from defects.

II. RESULTS

A. Experimental confirmation of diamagnetic property increases after H_{c1}

Figure 1 shows magnetization behaviors of two different (Fe, Ti) particle-doped MgB_2 specimens with various temperature, which are fabricated by perfectly same condition except for dopant level of (Fe, Ti) particles. Figure 1 (a) is magnetization behaviors of 5 wt.% (Fe, Ti) particle-doped MgB_2 (5 wt.% specimen) and shows different H_{c1} with various temperature. The deviation point from the linear line is the H_{c1} . Calculated roughly from the figure, H_{c1} of 5 wt.% specimen at 0 K is almost same as that at 5 K, which is 600 Oe. Figure 1 (b) is magnetization behaviors of 25 wt.% (Fe, Ti) particle-doped MgB_2 (25 wt.% specimen) with various temperatures. Their behaviors are similar with that of 5 wt.% specimen in the viewpoint that diamagnetic property increases after H_{c1} .

On the other hand, H_{c1} of 25 wt.% specimen at 0 K is about 500 Oe which is rather lower than the one of 5 wt.% specimen. The decrease of H_{c1} can be interpreted as a disturbance of the circulating current by over-doping of (Fe, Ti) particle. M-H curves of 5 wt.% specimen and 25 wt.% specimen to 3 kOe are shown in Fig. 1 (c) and (d), respectively. After reaching H'_{c1} in both figures, it is observed that $\Delta H = \Delta B$ regions are approaching [18]. In a VDS, it is our assertion that the diamagnetic property does not decrease after reaching the maximum diamagnetic property, but decreases after forming the $\Delta H = \Delta B$ section. Figure 1 (c) and (d) support the assertion.

B. A theoretical view of H'_{c1}

When magnetic field is applied on the superconductor, which has m^3 volume defects of radius r as shown in Fig. 2 (a), quantum fluxes are pinned on the defects after H_{c1} as shown Fig. 2 (b), (c), and (d). When the magnetic field of H_c is applied, the number of quantum

fluxes (n^2) pinned at a defect of radius r in the static state is

$$n^5 - \frac{2H_c^2}{\alpha} r^4 = 0 \quad (1)$$

where α is $\frac{aLA\Phi_o}{Pc}$. Φ_o is flux quantum which is 2.07×10^{-7} G·cm², c is the velocity of light, aL is an average length of quantum fluxes which are pinned and bent between defects (a is an average bent constant, $1 < a < 1.2$), A is 0.103 A (Ampere) and P is the filling rate which is $\pi/4$ when flux quanta are pinned at the defect in the form of square.

The equation shows how many quantum fluxes are pinned at a volume defect of which radius is r in a superconductor when magnetic field is applied. In reality, numbers of quantum flux pinned at a spherical volume defect of radius r is n^2 . The full version of deriving the Eq. (1) is shown in Method. We postulate our theory in the assumption that quantum fluxes pinned on the volume defect in the superconductor are picked out from the defect and move an inside of the superconductor due to two following reasons. The one is when pick-out forces of pinned fluxes are larger than the pinning force of the defect ($F_{pickout} > F_{pinning}$). And the other is when the minimum distance between quantum fluxes pinned at the defect are the same as that of H_{c2} . The justification of the latter came from the fact that there is no flux pinning effect if the neighborhoods of a defect is not a superconducting state anymore.

Deviating from the H_{c1} linear line means that fluxes penetrate into the inside of superconductor. And an increase of diamagnetic property after H_{c1} means that fluxes having penetrated are pinned at the defects and block the external field. The diamagnetic property of H'_{c1} would continue increasing as H is increasing if there are a lot of volume defect. It is because penetrated fluxes still remain near the surface of superconductor due to a lot of volume defects. However, we noticed that there is a limit of pinned fluxes on a defect, which is that fluxes pinned on a defect definitely move into an inside of the superconductor if the distance (d') between quantum fluxes pinned at the defect is the same as the one of the H_{c2} regardless of ΔG_{defect} .

H'_{c1} is the field that the fluxes pinned at the defect have to move regardless of ΔG_{defect} . Experimentally, the H'_{c1} on the M-H curve appears as a vertex or as a broad region. In most of superconductors, the H'_{c1} is the vertex of M-H curve, but some of the VDS shows a broad region of H'_{c1} in the M-H curve if volume defects in the superconductor is appropriate [18–20]. In our experiment, it is clearly observable in Fig. 1 (c) and (d). After reaching

H'_{c1} in both figures, it is observed that the $\Delta H = \Delta B$ region which means broad H'_{c1} are approaching [18].

Since the fluxes are pinned at defects and cannot move an inside of superconductor, it is natural that diamagnetic property increases. Penetrating behaviors of magnetic fluxes to H'_{c1} in the ideal state are explained in Fig. 3. They are calculated in the condition that the number of defects, of which radius is $0.163\mu\text{m}$, are 4000^3 in 1 cm^3 . H_{c1} and H_{c2} are assumed as 400 Oe and 50 Tesla (T), respectively [18]. When H is raised to 450 Oe, calculated max-pinning numbers of quantum fluxes of a defect are 28^2 and penetrated quantum fluxes are pinned to third defects from the surface. According to an increase of applied field (H), penetrated quantum fluxes are going not only to move another pinning site, but to increase the number of pinned fluxes on defects. Each volume defect which has pinned fluxes reaches its pinning limit ($n^2=45^2$) when H is 1435 Oe which is H'_{c1} , as shown in Fig. 3 (e). More H induces the $\Delta H = \Delta B$ region because pinning sites already reached their pinning limit (Fig. 3 (f)).

C. The pinning force of a defect, the pinning penetration depth at H'_{c1} , and magnetization

The pinning force of a defect (f_r) at H'_{c1} is calculated from Eq. (15) in Method by inserting the number of flux quanta (n) of Eq. (1) when Q is zero and shown in the Fig. 4 (a) and (b) under the condition that H_{c1} is 600 Oe. Figure 4 (a) is a pinning force distribution at H'_{c1} along the number of volume defects in the superconductor when the radius of defect is 163 nm. Despite the same size of defects, the pinning force of a defect shows a significant difference according to numbers of the defect. It is observed by calculation that the pinning force of a volume defect greatly increased as the number of volume defects decrease. Figure 4 (b) is a pinning force distribution at H'_{c1} along the number of volume defects in the superconductor when vol.% of the defects is fixed as 1.56. This is the case that the volume defects keep being divided to a smaller size. As the number of volume defects increases (their size decreases), the pinning force of a volume defect decreases dramatically.

Looking over the pinning penetration depth, which is defined as the depth of pinned fluxes on the defects in the superconductor at H'_{c1} in the ideal pinning state, the force which push the quantum fluxes into an inside of the superconductor by external field must be equal

to the sum of the bulk pinning force by Meissner effect and pinning forces of defects existing from the surface of the superconductor. It is assumed that quantum fluxes are penetrating into the superconductor along x-axis (quantum fluxes are laid on the y-axis) and an yz plane has m'^2 defects as shown Fig. 2 (a) and (b).

$$\frac{\partial(G_{H'_{c1}} - G_{H_{c1}})}{\partial m} = mm'^2 f_r \quad (2)$$

where f_r is the pinning force of a defect of which radius is r and m is the number of defects which have pinned fluxes to the flux movement direction. Thus,

$$\frac{H'^2_{c1} - H^2_{c1}}{8\pi} = \frac{m^2}{2} m'^2 f_r \quad (3)$$

Therefore, the pinning penetration depth of the specimen at H'_{c1} is $x = mL$. Calculated pinning penetration depths for the various states are shown in Fig. 4 (c) and (d) under the condition that H_{c1} is 600 Oe. Figure 4 (c) is the calculated pinning penetration depths at H'_{c1} along the number of volume defect when the radius of defect is 163 nm. It is observed that the pinning penetration depth increases as the number of volume defects decreases. A calculated pinning penetration depths at H'_{c1} along the number of volume defect when the vol.% of the defects is set as 1.56 are shown in Fig. 4 (d). At the same vol.% of the defects, the fluxes do penetrate deeply at H'_{c1} as the radius of defect increases.

The magnetic induction in the superconductor which have m'^3 volume defects is

$$B = n^2 m_{cps} m \Phi_o \quad (4)$$

where n^2 , m_{cps} , and m are the number of quantum fluxes pinned at a defect, the number of defect which is vertically closed packed state, and the number of defect which had pinned fluxes from the surface of the superconductor along x-axis as shown in Fig. 2 (a), respectively. The m_{cps} is the minimum number of defects if fluxes penetrated into the superconductor are completely pinned [18]. Thus, the total numbers of flux quanta pinned on defects of a plane perpendicular to the flux moving direction are $n^2 m_{cps}$. Magnetization M at H'_{c1} is

$$M = \frac{B - H}{4\pi} = \frac{n^2 m_{cps} m \Phi_o - H}{4\pi} \quad (5)$$

Calculated magnetizations at H'_{c1} in the static state along the applied field for various conditions are shown in Fig. 5.

III. DISCUSSION

The number of flux quanta pinned on volume defects have been calculated in a static state. However, two terms are added in the dynamic state. Since the fluxes are approaching volume defects with their velocity, there would be a kinetic energy. And there would be a vibration energy because fluxes pinned on the volume defects are continuously vibrating. Magnetic quantum fluxes can be classified as pinned parts at the volume defect and unpinned parts in superconductors, and the latter are continuously affected by other fluxes movements. Thus, the former continue to vibrate because they are interconnected. Therefore,

$$\Delta G_{pickout} = \Delta G_{defect} - (\Delta K.E. + \Delta G_{vibration}) = \Delta G_{defect} - \Delta G_{dynamic} \quad (6)$$

As the distance between the volume defects increases, $\Delta K.E.$ increase because a large velocity of the fluxes is induced when they are picked out from the defect. And $\Delta G_{vibration}$ increase as the number of flux quanta pinned at a volume defect increase. Thus, as the radius of volume defect increases, flux quanta will be picked out from the volume defect at a much fewer flux quanta than that of the static state.

On the other hand, as the radius of volume defect decreases and the number of it increases, $\Delta G_{dynamic}$ decreases. Flux quanta penetrated into the superconductor from the outside, are pinned on the volume defects around the surface, and move into an inside of superconductor before the number of them becomes larger as shown Fig. 3 and are pinned again on the next volume defect. Thus, the diamagnetic property at H'_{c1} is not greatly increased because a pinning limit of the volume defects is low as shown Fig. 5 (e) and (f). And the degree of bending of the fluxes is also low because the distance between the defects is not wide and their pinning limit is low. Therefore, $\Delta G_{dynamic}$ is small.

Another problem that breaks the increase of the diamagnetic property in superconductors is the flux jump. What the number of fluxes pinned at a volume defect increases means that the number of fluxes moving together also increase because they are moving together when they are picked out from the defect, which results in generating a lot of heat, and it means the degradation of the superconductor. The maximum diamagnetic property of the pure specimen at 5 K is approximately -100 emu/cm³, which is shown in Fig. 6 (a). The maximum diamagnetic property of pure MgB₂ would increase more at 5 K if there were no flux jump. As shown in Fig. 6 (b), it is observed that a higher diamagnetic property appears

at 10 K, which is close to -150 emu/cm^3 when a magnetic field in the opposite direction is applied. Generally, as the temperature of a superconductor decreases, the diamagnetic property increases. If there were no flux jump at 5 K, it is clear that the diamagnetic property at 5 K would be greater than 10 K.

We used 96.6 wt.% purity of the boron in synthesizing pure MgB_2 , and the impurity of 3.4 wt.% are equal to approximately 1.3 vol.% in MgB_2 . It produced volume defects of which radius is $1 \mu\text{m}$ on average, as shown in Fig. 6 (e). In reality, the diamagnetic property would continue to increase over 5000 Oe although H_{c1} of the specimen is approximately 400 Oe. The calculated max-diamagnetic property of the superconductor in the static state, which contains defects of which radius is $1 \mu\text{m}$ and its vol.% is 1.56, is -456.6 emu/cm^3 at 0 K (H'_{c1} is 6370 Oe), as shown in Fig. 5 (c) and (d). As the number of volume defects which had pinned fluxes increases, the number of flux quanta pinned at a volume defect increases up to 276^2 , which is its pinning limit. However, this phenomenon does not happen because influences $\Delta G_{dynamic}$ and flux jump are severe in the pure MgB_2 . In our calculation by Eq. (5), maximum 135^2 flux quanta would be pinned at $1 \mu\text{m}$ volume defects if the max-diamagnetic property have occurred at 5000 Oe in the pure MgB_2 . And it is observed that they cause a flux jump before reaching H'_{c1} as shown in Fig. 6 (a).

On the other hand, when (Fe, Ti) particles are doped on MgB_2 , pinned fluxes have much less opportunity to move a large distances because the (Fe, Ti) particles are pinning the fluxes together with $1 \mu\text{m}$ radius defects, as shown in Fig 2 (d). We used (Fe, Ti) particles of which radius is 163 nm on average as the dopant as shown in Fig. 6 (d). 5 wt.% (Fe, Ti) particles in MgB_2 corresponds to approximately 2.5 vol.% in MgB_2 and means that MgB_2 has approximately 8000^3 volume defects. If there were no defects of which radius is $1 \mu\text{m}$ in the superconductor, the calculated diamagnetic property cannot exceed -52 emu/cm^3 , as shown in Fig. 5 (a) and (b). However, the diamagnetic property of the 5 wt.% specimen, which exceed -150 emu/cm^3 , is considered as the effect of defects of which radius $1 \mu\text{m}$ on average.

Using Eq. (1), we get $n^2 = 289^2$ for $1 \mu\text{m}$ radius defect when the distance between the volume defects in pinned state is $3.9 \mu\text{m}$ and H'_{c1} is 2000 Oe ($L' = 3.9 \mu\text{m}$, which is comparable with $L' = 50 \mu\text{m}$ of pure MgB_2). This exceeds the maximum pinning limit of $1 \mu\text{m}$ radius defect, which is 276^2 , thus $1 \mu\text{m}$ radius defect can pin the fluxes up to 276^2 ones. On the other hand, we can calculate the number of pinned fluxes at $1 \mu\text{m}$ radius defect from

the diamagnetic property of the specimen at 2000 Oe by using Eq. (5). It was considered that m is 1 because that 1 μm radius defect can pin up to 276^2 fluxes and 0.163 μm radius defect can pin up to 45^2 ones, which are scattered around the defect of 1 μm radius. Fluxes pinned at the defect of 1 μm radius are picked out when 230^2 fluxes are pinned at the defect. Therefore, $\Delta G_{dynamic}$ for 1 μm of 5 wt.% (Fe, Ti) particle-doped MgB_2 specimen is much smaller than that of the pure MgB_2 .

On the other hand, calculating n^2 of 163 nm radius defect by Eq. (1) under the same conditions ($L'=3.9 \mu\text{m}$ and $H'_{c1}=2000$ Oe), we get 68^2 . However, it has pinning limit that is 45^2 , which is caused by H_{c2} . Thus, the difference between the number of pinned fluxes calculated from the free energy relation and the pinning limit by H_{c2} is considerable at H'_{c1} , which is much larger than that of 1 μm radius defect. $\Delta G_{dynamic}$ is also small because 163 nm radius defect can pin small number of quantum fluxes (45^2). Therefore, the number of fluxes pinned at 163 nm radius defect is hardly affected by $\Delta G_{dynamic}$.

IV. CONCLUSION

We experimentally showed the increase of magnetization by flux pinning effect by the specimens which are a volume defect-dominating superconductor. And we theoretically proved the phenomenon by modeling. We represented that there is a new critical field called H'_{c1} which is defined as a field showing the maximum diamagnetic property in the superconductor. As a results of calculation, H'_{c1} depends on the size and the number of defects causing the flux pinning. When volume defects are large and a few, the experimental results are much lower than the calculated ones because of a large $\Delta G_{dynamic}$ and flux jump. However, when volume defects are small and many, the results are closer to the calculated ones because of a small $\Delta G_{dynamic}$.

V. METHOD

A. Experiment

(Fe, Ti) particle-doped MgB_2 specimens were synthesized using the non-special atmosphere synthesis (NAS) method [21]. The starting materials were Mg (99.9% powder) and B (96.6% amorphous powder) and (Fe, Ti) particles. Mixed Mg and B stoichiometry, and

(Fe, Ti) particles were added by weight. They were finely ground and pressed into 10 mm diameter pellets. (Fe, Ti) particles were ball-milled for several days, and average radius of (Fe, Ti) particles was about $0.163 \mu\text{m}$. On the other hand, an 8 m-long stainless- steel (304) tube was cut into 10 cm pieces. One side of the 10 cm-long tube was forged and welded. The pellets and excess Mg were placed in the stainless-steel tube. The pellets were annealed at $300 \text{ }^\circ\text{C}$ for 1 hour to make them hard before inserting them into the stainless-steel tube. The other side of the stainless-steel tube was also forged. High-purity Ar gas was put into the stainless-steel tube, and which was then welded. Specimens had been synthesized at $920 \text{ }^\circ\text{C}$ for 1 hour and cooled in air. Field dependences of magnetization were measured using a MPMS-7 (Quantum Design). During the measurement, sweeping rates of all specimens were made equal for the same flux-penetrating condition.

B. A full derivation of the equation

If the field H_{c1} is applied to the superconductor, the free energy (FE) density of the superconductor will be raised to $\Delta G_s = H_{c1}^2/8\pi$. On the other hand, the FE density of the defects in the superconductor will be $\Delta G_n = 0$ at H_{c1} because there is no fluxes in the defects and they are not superconductor. Magnetic fluxes which is in the state of flux quantum begin to penetrate into the specimen beyond the H_{c1} through the surface of the superconductor. Quantum fluxes which have penetrated into the superconductor are willing to move to the inside of specimen by a concentration gradient of quantum fluxes and repulsive force between them, and will be pinned at the defect where the FE density is lower than the one of superconductor. In this situation, the fluxes penetrated into the superconductor are pinned at the defect around the surface of the superconductor if volume defects are appropriate, thus the amount of the fluxes penetrated into the superconductor is a few enough to ignore. If it is assumed that the applied field is raised to H_c which is parallel to the specimen surface, the FE density difference between superconductor and the defect is

$$\Delta G_n - \Delta G_s = -\frac{H_c^2}{8\pi} \quad (7)$$

Therefore, the free energy density of a spherical defect is

$$\Delta G_{defect} = -\frac{H_c^2}{8\pi} \times \frac{4}{3}\pi r^3 + \Delta\epsilon_n \times 2r \quad (8)$$

where H_c is the applied field, r is a radius of defect and $\Delta\epsilon_n$ is the free energy density increase of the defect by fluxes which are pinned at it. Since the fluxes in the superconductor exist in the form of quantum fluxes, they have vortexes of eddy currents. Hence $\Delta\epsilon_n$ is $n^2\Phi_o^2/8\pi$, where n is number of flux quanta pinned at the defect and the flux quantum Φ_o is $2.07\times 10^{-7}\text{G}\cdot\text{cm}^2$. Multiplying $2r$ to $\Delta\epsilon_n$ in Eq. (2) means that the FE density of a defect increases as much as $2r$ in the pinned quantum fluxes. Looking at the depth of FE density of a defect, it is entirely dependent on the volume of the defect.

On the other hand, total forces acting on fluxes pinned at the defect are a softened pinning force by quantum fluxes stacked on the defect and the tension forces acting between a pinned part and an unpinned part in quantum fluxes on the defect. The tension force of the forefront flux quantum in two dimensions (2 D), as shown in Fig. 2 (c), is the number of quantum fluxes which are pinned at the defect times a repulsive force acting between quantum fluxes. The repulsive force per unit length (cm) between quantum fluxes, which is caused by vortexes, is

$$f = J_s \times \frac{\Phi_o}{c} \quad (9)$$

where J_s is supercurrent density perpendicular to the flux-flow [22]. Assuming that n of quantum fluxes are pinned between two defects which distance is L , the tension force on the forefront of the quantum fluxes is

$$f_{tension} = aLnJ_s \times \frac{\Phi_o}{c} \quad (10)$$

where n is the number of quantum fluxes which are pinned horizontally at the defect, aL is a average length of quantum fluxes which are pinned and bent between defects (a is average bent constant, $1 < a < 1.2$) and J_s can be expanded to total supercurrent density. These behaviors are explained in Fig. 2 (b) and (c).

In addition, a quantum flux tension of which is pinned between the defects can be described as a behavior of Hook's law

$$f_{tension} = -kx \quad (11)$$

where k is a quantum flux tension constant and x is the displacement along the x-direction from the center between defects which pinned quantum fluxes to the forefront quantum flux as shown in Fig. 2 (c). The displacement x can be written as

$$x = nd, d = \frac{\sum_{n=1}^n d_n}{n} \quad (12)$$

where d_n is the maximum distance among distances between pinned fluxes as defined in the Fig. 2 (b). Therefore, the extended vortex tension constant k is

$$k = \frac{aLJ_s\Phi_o}{dc} \quad (13)$$

On the other hand, there might be fluxes which are not pinned at any defect when the distance between defects is wide enough. These unpinned fluxes would be present in a compressed state because there are pinned fluxes before them. Thus, they cause the pushing force ($F_{pushing}$) to push pinned fluxes forward and assumed to be a product of pinned fluxes.

Quantum fluxes pinned at the defect begin to move by being picked out if the pinning force and the pushing plus tension forces are same. Thus,

$$\Delta F_{pinning} = \frac{\partial G}{\partial r} = -\frac{H_c^2}{8\pi} \times 4\pi r^2 + \frac{2n^2\Phi_o^2}{8\pi} \quad (14)$$

and we assumed that Q times fluxes of the number of fluxes pinned at a defect exist between defects in the compressed state,

$$\Delta F_{pickout} = -Qn_vLnJ_{s1}\frac{\Phi_o}{c} - n_v \sum_{n=1}^n kx_n = -Q\frac{LJ_{s1}\Phi_o}{c}n^2 - \frac{aLJ_s\Phi_o}{2c}n^3 \quad (15)$$

where J_{s1} is the current density of circulating flux quantum in a compressed state. It was assumed that the distance between quantum fluxes pinned at the defect to the vertical direction is the same as that of horizontal direction and n_v (the number of quantum fluxes vertically pinned at the defect) is same as n , fluxes pinned at the defect are vertically subjected to the same tension. They will move into an inside of the superconductor if $\Delta F_{pickout}$ is larger than $\Delta F_{pinning}$.

$$-\frac{H_c^2}{8\pi} \times 4\pi r^2 + \frac{2n^2\Phi_o^2}{8\pi} = -Q\frac{LJ_{s1}\Phi_o}{c}n^2 - \frac{aLJ_s\Phi_o}{2c}n^3 \quad (16)$$

On the other hand, the critical current density (J_c) between two flux quanta can be calculated as Silsbee criterion [23].

$$J_c = \frac{c}{4\pi} \frac{N\Phi_o}{d'/2} \leq \frac{c}{2\pi} \frac{H_{c2}}{d'} \quad (17)$$

where N is the number of flux quantum in the superconductor and d' is the minimum distance between quantum fluxes pinned at the defect, which is shown in Fig. 2 (b). J_c is the maximum at H_{c2} .

Since the repulsive force between flux quanta are inversely proportion to r^2 (r is the distance between the flux quanta), the J_c of eddy current circulating the flux quantum are also inversely proportion to $(d')^2$ by Eq. (11). If maximum current density is set as a boundary, $J_{s,d'}$ is

$$J_{s,d'} = \frac{A}{(d'/2)^2} = \frac{An^2}{Pr^2} \quad (18)$$

where A is constant, which is 0.103 A (Ampere), r is the radius of defect, n^2 is the number of quantum flux pinned at the defect and P is filling rate which is $\pi/4$. During the calculation, $d'/2$ is derived from the following equation when flux quanta are pinned at the defect in the form of square [18].

$$n^2 = \frac{\pi r^2}{\pi(\frac{d'}{2})^2} \times P \quad (19)$$

The average value of J_s between d and d' have to be inserted at the equation (22), which is almost $J_{s,d'}/2$. Thus, assuming that J_{s1} is $\frac{1}{3}J_{s,d'}$, the equation is

$$\frac{aLA\Phi_o}{4Pc}n^5 + Q\frac{LA\Phi_o}{3Pc}n^4 - \frac{H_c^2}{8\pi} \times 4\pi r^4 = 0 \quad (20)$$

The term $\frac{2n^2\Phi_o^2}{8\pi}$ can be ignored owing to Φ_o^2 . Putting $\alpha = \frac{aLA\Phi_o}{Pc}$

$$n^5 + \frac{4Q}{3a}n^4 - \frac{2H_c^2}{\alpha}r^4 = 0 \quad (21)$$

When Q is zero

$$n^5 - \frac{2H_c^2}{\alpha}r^4 = 0 \quad (22)$$

Acknowledgment

The authors would like to thank Dr. B. J. Kim of PNU for careful discussion.

-
- [1] Michael Tinkham, *INTRODUCTION TO SUPERCONDUCTIVITY*, Dover pub. Mineola, **2nd** 149-162 (2004).
 - [2] Y. Radzyner, A. Shaulov, Y. Yeshurun, I. Felner, K. Kishio, and J. Shimoyama, Anisotropic order-disorder vortex transition in $\text{La}_{2-x}\text{A}_x\text{Sr}_x\text{CuO}_4$. *Phys. Rev. B* **65** 214525 (2002)
 - [3] S. Salem-Sugui et al. Flux dynamics associated with the second magnetization peak in the iron pnictide $\text{Ba}_{1-x}\text{K}_x\text{Fe}_2\text{As}_2$. *Phys. Rev. B* **82** 054513 (2010)
 - [4] H. B. Lee, G. C. Kim, Y. C. Kim and D. Ahmad. Flux jump behaviors and mechanism of FeTi doped MgB_2 at 5 K. *Physica C* **515** 31-35 (2015).
 - [5] Babar Shabbir, Xiaolin Wang, Y. Ma, S. X. Dou, S. S. Yan, and L. M. Me, Study of flux pinning mechanism under hydrostatic pressure in optimally doped (Ba,K) Fe_2As_2 single crystals. *Sci. Rep.* **6** 23044 (2016).
 - [6] Mika Malmivirta et al. Enhanced flux pinning in YBCO multilayer films with BCO nanodots and segmented BZO nanorods. *Sci. Rep.* **7** 14682 (2017)
 - [7] Wei Zhou, Xiangzhuo Xing, Wenjuan Wu, Haijun Zhao, and Zhixiang Shi, Second magnetization peak effect, vortex dynamics, and flux pinning in 112-type superconductor $\text{Ca}_{0.8}\text{La}_{0.2}\text{Fe}_{1-x}\text{Co}_x\text{As}_2$. *Sci. Rep.* **6** 22278 (2016).
 - [8] I N Askerzade, A Gencer, N Güçlü, and A Kihc, Two-band Ginzburg-Landau theory for the lower critical field H_{c1} in MgB_2 . *Supercond. Sci. Technol.* **15** L17-L20 (2002).
 - [9] Cristina Buzea and Tsutomu Yamashita, Review of superconducting properties of MgB_2 . *Supercond. Sci. Technol.* **14** R115-R146 (2001).
 - [10] S. L. Li et al. Linear temperature dependence of lower critical field in MgB_2 . *Phys. Rev. B* **64** 094522 (2001)
 - [11] C. D. Wei, Z. X. Liu, H. T. Ren, and L. Xiao, Fishtail effects in $\text{YBa}_2\text{Cu}_3\text{O}_y$ crystal prepared by melt-textured growth method. *Physica C* **260** 130-136 (1996).
 - [12] C S Yadav and P L Paulose, Upper critical field, lower critical field and critical current density of $\text{FeTe}_{0.60}\text{Se}_{0.40}$ single crystals. *New J. Phys.* **11** 113046 (2009).

- [13] Anupam, P L Paulose, S Ramakrishnan and Z Hossain, Doping dependent evolution of magnetism and superconductivity in $\text{Eu}_{1-x}\text{K}_x\text{Fe}_2\text{As}_2$ ($x=0-1$) and temperature dependence of the lower critical field H_{c1} . *J. Phys.: Condens. Matter* **23** 455702 (2011).
- [14] H Yamasaki and K Endo, Nanostructural defects for effective flux pinning in high quality $\text{Bi}_2\text{Sr}_2\text{CaCu}_2\text{O}_{8+x}$. *Supercond. Sci. Technol.* **27** 025014 (2014).
- [15] C. P. Bean and J. D. Livingston, Surface barrier in type-II superconductor. *Phys. Rev. Lett.* **12** 14 (1964).
- [16] K. Westerholt, B. vom Hedt, and H. Bach, Flux Penetration and Bean-Livingston Barriers in $\text{Bi}(2212)$ Single Crystals. *Physica B* **194** 1907 (1994).
- [17] M. Konczykowski, L. I. Burlachkov, Y. Yeshurun, and F. Holtzberg, Evidence for surface barriers and their effect on irreversibility and lower-critical-field measurements in Y-Ba-Cu-O crystals. *Phys. Rev. B* **43** 13707 (1991).
- [18] H. B. Lee, G. C. Kim, H. J. Park, D. Ahmad, and Y. C. Kim, $\Delta H = \Delta B$ region in volume defect-dominating superconductors. <https://arxiv.org/abs/1805.04683v1> (2017)
- [19] S. W. Hsu, K. Chen, and W. H. Lee, Temperature and Field-Sweeping Rate Dependence of Flux Jumps in A Melt-Textured $\text{YBa}_2\text{Cu}_3\text{O}_{7-x}$ Superconductor. *Solid State Communications* **75** 799 (1990).
- [20] K. H. Müller and C. Andrikidis, Flux jumps in melt-textured Y-Ba-Cu-O, *Phys. Rev. B* **49**, 1294-1307 (1994).
- [21] H. B. Lee, Y. C. Kim and D. Y. Jeong, Non-special atmosphere synthesis for MgB_2 . *J. Kor. Phys. Soc.* **48** 279-282 (2006).
- [22] Michael Tinkham, *INTRODUCTION TO SUPERCONDUCTIVITY*, Dover pub. Mineola, **2nd** 1-42 (2004).
- [23] Michael Tinkham, *INTRODUCTION TO SUPERCONDUCTIVITY*, Dover pub. Mineola, **2nd** 21 (2004).

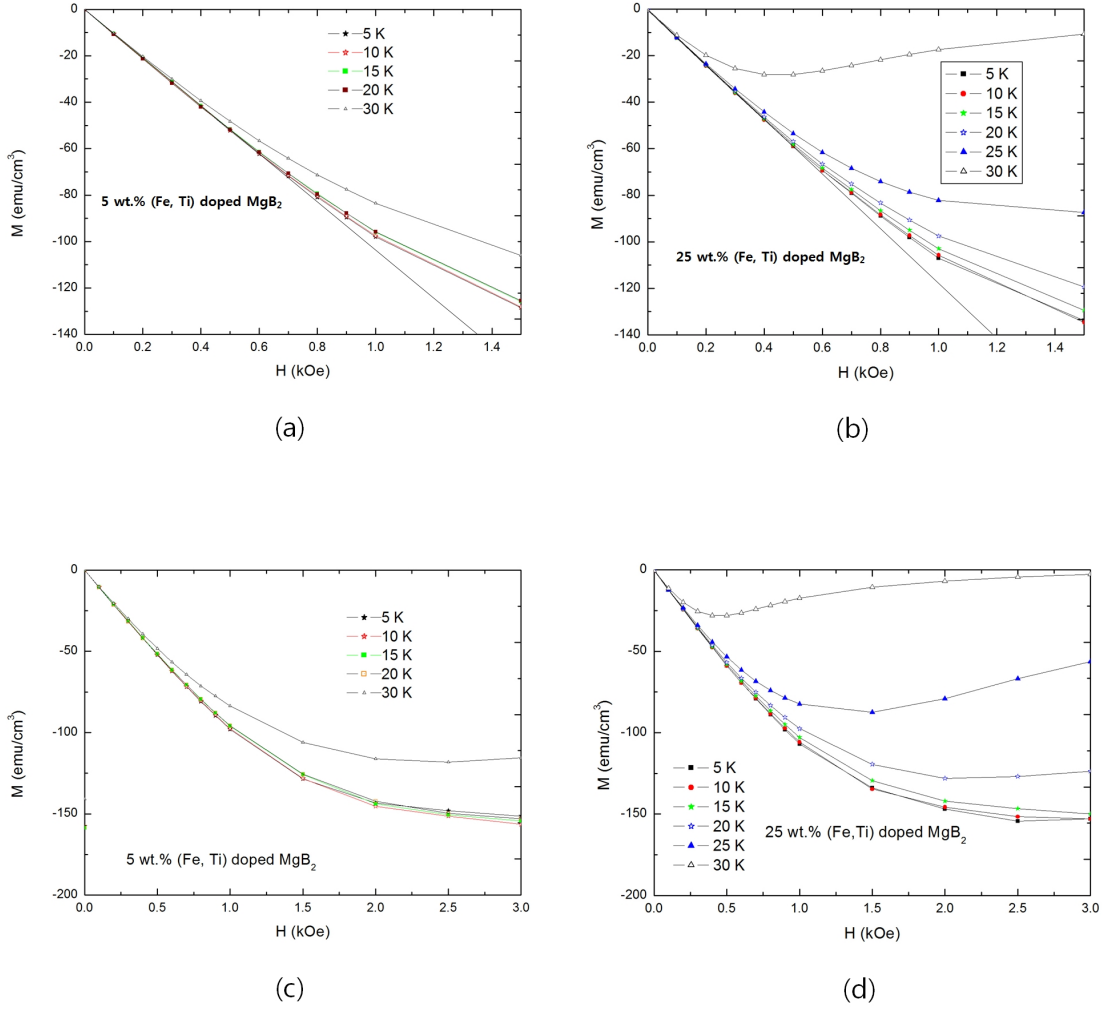


FIG. 1: Magnetization behaviors of volume defects-dominating superconductors around H_{c1} . Deviation point from the linear line is the H_{c1} . (a): Magnetization behaviors of 5 wt.% (Fe, Ti) particle-doped MgB₂ with various temperature. It is determined that H_{c1} is around 600 Oe at 0 K. (b): Magnetization behaviors of 25 wt.% (Fe, Ti) particle-doped MgB₂ with various temperature. It is determined that H_{c1} is around 500 Oe at 0 K, which is rather lower than the one of 5 wt.% (Fe Ti) doped MgB₂. The diamagnetic property increases after H_{c1} are shown in both specimens. (c): Magnetization behaviors of 5 wt.% (Fe, Ti) particle-doped MgB₂ which are extended to 3.0 kOe. (d): Magnetization behaviors of 25 wt.% (Fe, Ti) particle-doped MgB₂ which are extended to 3.0 kOe. It is observed that (c) and (d) both have a broad H'_{c1} which means the $\Delta H = \Delta B$ section as external magnetic field H increases.

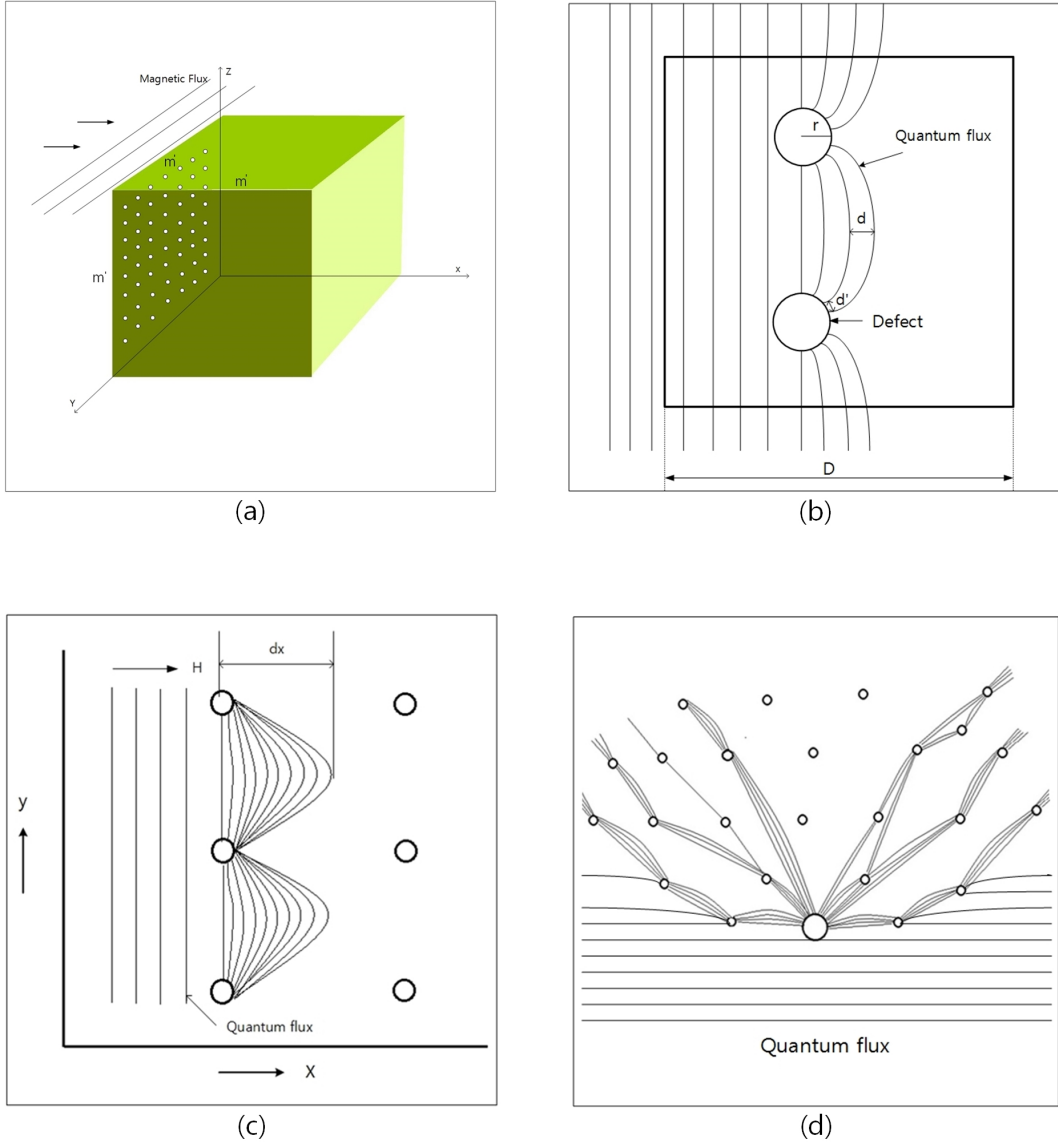


FIG. 2: Schematic representations of flux pinning on volume defects. (a): The distribution of defects in the superconductor. It is assumed that an each axis has m' defects of radius r in 1 cm^3 superconductor. If an external field exceeds H_{c1} , penetrated fluxes are pinned from the surface of the superconductor. (b): A definition of d and d' . (c): An image of several quantum fluxes pinned on defects simultaneously. Fluxes coming from the outside into the superconductor in the form of quantum fluxes are pinned at a defect having a relatively lower free energy. (d): An image that fluxes are pinned on several defects simultaneously when large and small defects are present together in the superconductor.

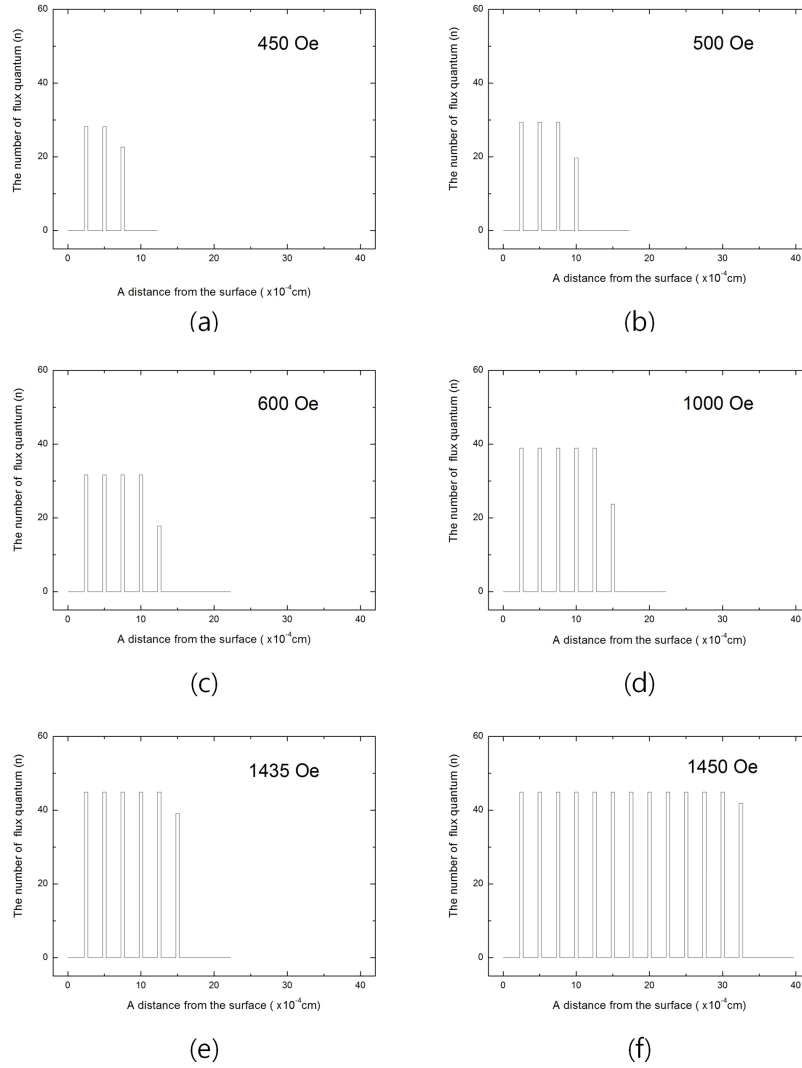


FIG. 3: Pinned fluxes penetration methods, pinning penetration depths and the number of flux quantum pinned at the defect in variation with the applied field for 4000^3 defects of $0.163 \mu\text{m}$ radius in 1 cm^3 . The vol.% of defects is 0.29, H_{c1} is 400 Oe and calculated H'_{c1} is 1435 Oe. (a): Calculated the number of quantum fluxes along the pinning site when H is 450 Oe. Penetrated fluxes are pinned to third pinning sites. (b): Calculated quantum fluxes when H is 500 Oe. Fluxes penetrated and are pinned to fourth pinning sites. The number of fluxes that can be pinned at a pinning site is larger than that at 450 Oe. (c): Calculated quantum fluxes when H is 600 Oe. (d): Calculated quantum fluxes when H is 1000 Oe. (e): Calculated quantum fluxes when H is 1435 Oe. Each pinning sites reach its pinning limit. (f): Calculated quantum fluxes when H is 1450 Oe. $\Delta H = \Delta B$ region are formed because pinning sites already reached their pinning limit.

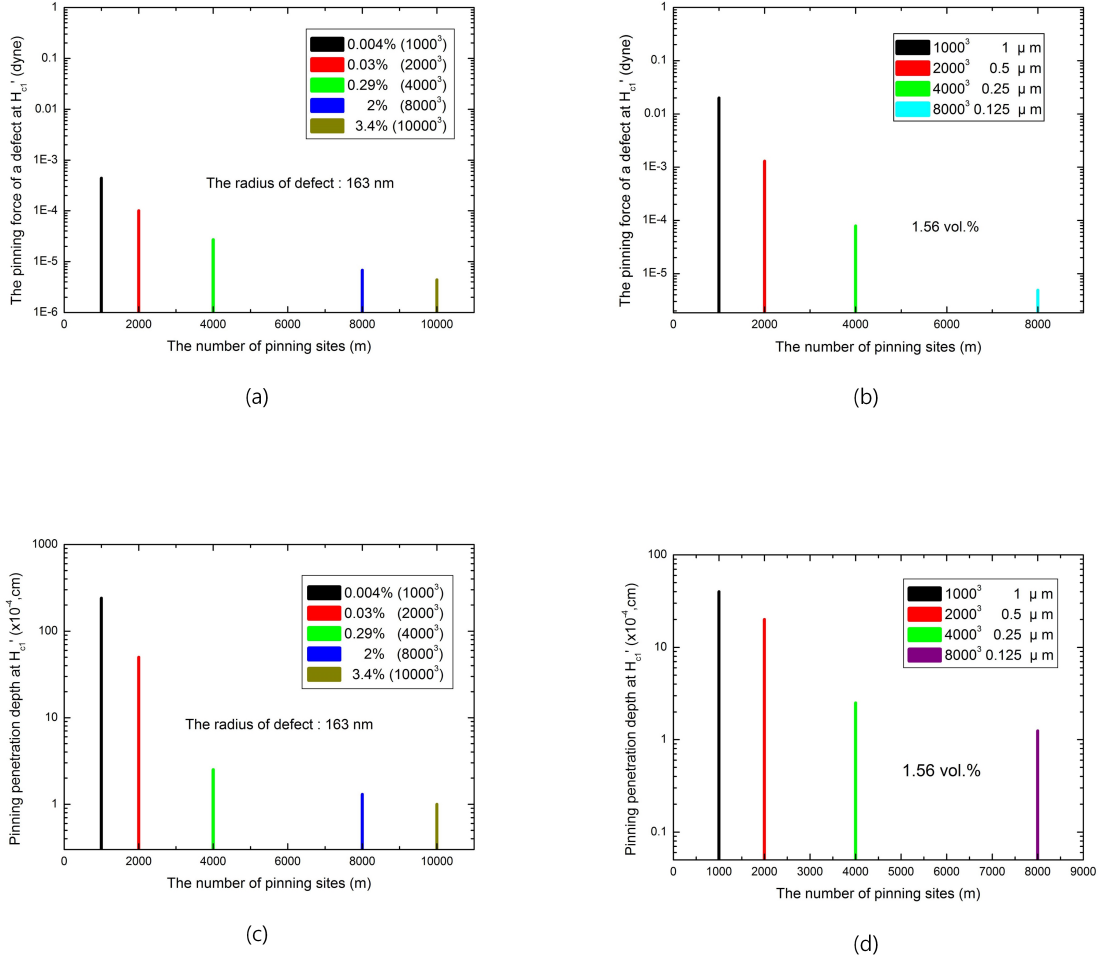


FIG. 4: Pinning forces of a volume defect at H'_{c1} and pinning penetration depth at H'_{c1} when H_{c1} is 600 Oe. (a): Calculated pinning forces of a volume defect at H'_{c1} along the number of defects when the radius of a defect is 163 nm. (b): Calculated pinning forces of a volume defect at H'_{c1} along the number of defects when the vol.% of the defects are 1.56. (c): Calculated pinning penetration depth of various conditions at H'_{c1} when the radius of a volume defect is 163 nm. (d): Calculated pinning penetration depth of various conditions at H'_{c1} when the vol.% of the defects are 1.56.

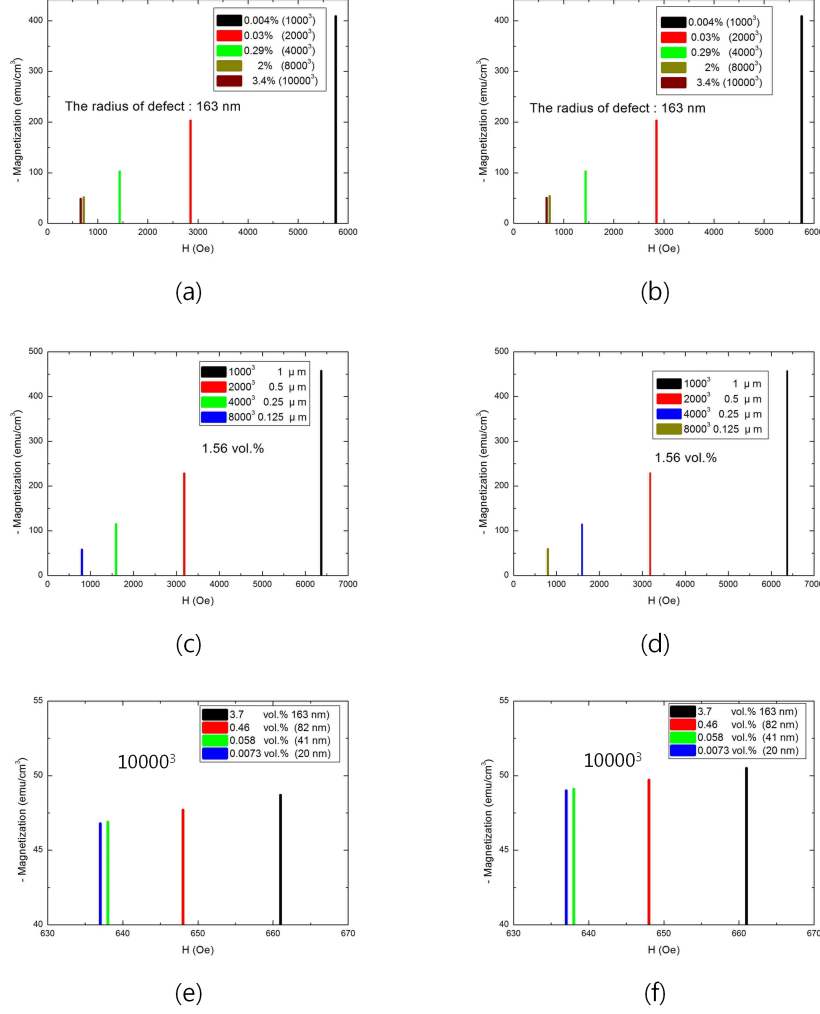
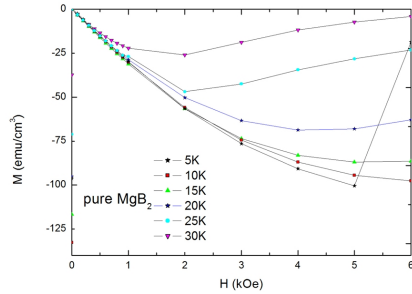
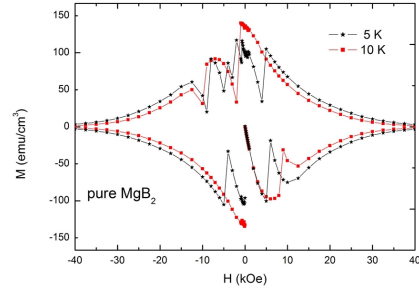


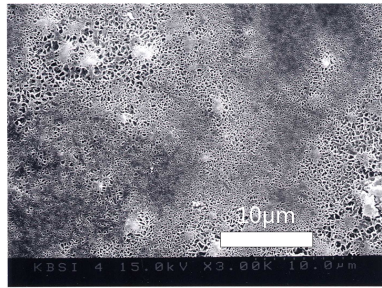
FIG. 5: Calculated magnetizations at H'_{c1} along the applied field for various conditions (a): Calculated magnetizations along the applied field at H'_{c1} when the radius of volume defects is 163 nm and H_{c1} is 400 Oe. (b): Calculated magnetizations at H'_{c1} when the radius of volume defects is 163 nm and H_{c1} is 600 Oe. (c): Calculated magnetizations at H'_{c1} when the concentration of volume defects is 1.56 vol.% and H_{c1} is 400 Oe. (d): Calculated magnetizations at H'_{c1} when the concentration of volume defects is 1.56 vol.% and H_{c1} is 600 Oe. (e): Calculated magnetizations at H'_{c1} for various vol.% of defects when the number of volume defects are fixed as 10000³ and H_{c1} is 400 Oe. (f): Calculated magnetizations at H'_{c1} for various vol.% of defects when the number of volume defects are fixed as 10000³ and H_{c1} is 600 Oe.



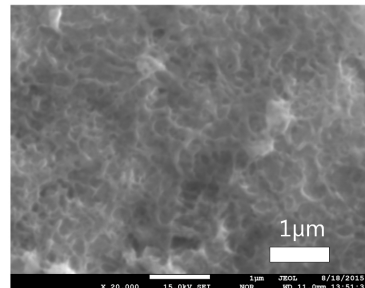
(a)



(b)



(c)



(d)

FIG. 6: M-H curves and photographs of pure and (Fe, Ti) particle-doped MgB_2 . (a): M-H curves of pure MgB_2 to 6 kOe. A flux jump was observed at 5 kOe on the M-H curve measured at 5 K. (b): Full M-H curves of pure MgB_2 at 5 K and 10 K. (c): A photograph of pure MgB_2 . The white bright ones in the MgB_2 base are volume defects. (d): A photograph of 5 wt.% specimen. (Fe, Ti) particles are observed in the MgB_2 base.